Agricultural and Forest Meteorology 320 (2022) 108942

Contents lists available at ScienceDirect

Agricultural and Forest Meteorology

journal homepage: www.elsevier.com/locate/agrformet

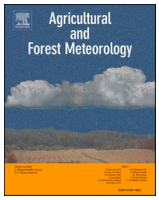

Reconstructing multi-decadal airborne birch pollen levels based on NDVI data and a pollen transport model

Willem W. Verstraeten [a,*], Rostislav Kouznetsov [b], Lucie Hoebeke [c], Nicolas Bruffaerts [c], Mikhail Sofiev [b], Andy W. Delcloo [a]

[a] Royal Meteorological Institute of Belgium, Ukkel, Brussels, Belgium
[b] Finnish Meteorological Institute, Helsinki, Finland
[c] Sciensano, Brussels, Belgium

ARTICLE INFO

Keywords:
Aerobiology
Birch pollen
Retrospective modelling, Chemistry transport model
NDVI

ABSTRACT

Airborne birch pollen may elicit allergies and affect the public health badly. Timely spatially distributed information on current and forecasted pollen levels may help people with pollen allergies to take preventive measures. This requires a modelling approach. Here we reconstruct multi-decadal (1982–2019) daily spatially distributed airborne birch pollen levels by ingesting seasonal dynamic birch pollen emission source maps into the pollen transport model SILAM (System for Integrated modeLling of Atmospheric coMposition) in a bottom-up approach. We introduce seasonal variations in the birch pollen emission maps by combining a forest inventory based areal birch fraction map with four decades of spaceborne Normalized Difference Vegetation Index (NDVI) in a Random Forest statistical framework. The approach of combining the transport model with NDVI based pollen emission maps is applied and evaluated with birch pollen observations by Hirst method from the Belgian aerobiological surveillance network that go back to 1982. Transport in SILAM is driven by ECMWF ERA5 meteorological data. The mean seasonal R^2 values between modelled and observed time series of airborne birch pollen levels in the period 1982–2019 range between 0.35 and 0.63, but can go up to 0.86 for individual seasons, indicating good performance of SILAM for Belgium. Here we show that the predicted amount of birch pollen in the air in Belgium has been increasing on average by 13.1% per decade based on the Sen slopes computed on the Seasonal Pollen Integral for the period 1982-2019. Analysis of the SILAM runs shows that this increase over time is mainly climate-induced (8.2% per decade), but it is amplified by the spatiotemporal variations of the birch pollen emission sources with 4.9% per decade.

1. Introduction

Life quality and life expectancy are largely affected by the long-term quality of air that we breathe in (Landrigan et al., 2017; Liu et al., 2019). Air contaminants such as VOCs, SO_X, NO_X, aerosols (EEA, 2017) deteriorate the air quality and may originate both from natural as well as from anthropogenic emission sources. Allergenic pollen, which are biogenic aerosols, may also affect the public health badly, especially in combination with long-term exposure by other air pollutants (D'Amato et al., 2007). More than 20% of the population in Europe suffers from pollinosis (WHO, 2003). Pollen allergies are on the rise globally, with worldwide approximately 10–30% of adults and 40% of children (Beggs, 2004; Bieber et al., 2016; Schmidt, 2016; Reitsma et al., 2018; Neumann et al., 2019). Bousquet et al., (2020) pointed to a large geographical variability within and between countries regarding pollen-associated allergic rhinitis, the most common disease phenotype. Looking at the whole spectrum of allergic symptoms that can be triggered by pollen exposure, it appears to be significantly different from one country to another (Baldacci et al., 2018). Over time, more and more people suffer from pollen allergies. For instance, allergic rhinitis was only sparsely reported in the late 1960's in Finland, while in the early 2000's more than 10% of the young men suffered from it (Latvala et al, 2005). This rise in pollen allergies is also reflected into a growing amount of published research Beggs (2021). In Belgium, a highly industrialized and densely populated country with substantial air pollution (Verstraeten et al., 2018), at least ~10% of the people develop allergic rhinitis symptoms due to birch tree pollen (Blomme et al., 2013). Before we can assess the impact of long-term exposure of air

* Correspondence author
E-mail address: Willem.Verstraeten@meteo.be (W.W. Verstraeten).

https://doi.org/10.1016/j.agrformet.2022.108942
Received 25 February 2022; Received in revised form 31 March 2022; Accepted 2 April 2022
Available online 19 April 2022

pollution and airborne allergenic pollen on the public health, the amount of allergenic pollen distributed over space and time must be quantified over a sufficient long period. Historical data on airborne pollen levels, available from aerobiological surveillance networks, are very useful but also are very sparse in time and particular in space. In particular, the only five monitoring stations located in Belgium may not be enough to address the spatial heterogeneity of pollen exposure in order to evaluate potential health risks at individual level (Stas et al., 2021a). Local landscape context is indeed known to drive the airborne tree pollen composition at specific distances from emission sources (Stas et al., 2021b).

Reconstructing spatiotemporal airborne birch pollen levels near the surface over a longer period requires data on vegetation dynamics connected with in-depth knowledge of processes on pollen release, transport and deposition under varying meteorological conditions. Among other modelling approaches to quantify airborne birch pollen levels (see also review of Maya-Manzano, et al., 2020), Chemistry Transport Models (CTM's) combine physical and biological laws and thus are powerful forecasting and hindcasting tools (Sofiev et al., 2015). Consequently, pollen transport models are suitable for reconstructing airborne birch pollen levels near the surface. Pollen transport models that are based on a bottom-up approach rely on coarse scale vegetation maps (Siljamo et al., 2013) derived from local inventory data. In such an approach maps of pollen emission sources are ingested by the CTM. These maps, however, may be outdated and lack inter-seasonal variations in birch pollen productivity (Siljamo et al., 2013, Hoebeke et al., 2018). The total amount of pollen during the pollen season is referred to as the Seasonal Pollen Integral (SPIn) (Siljamo et al., 2013, Gálan et al., 2017). The inter-seasonal variations of SPIn can be very important, especially for trees which present typical production cycles due to mast seeding (Clement et al., 2010; Hoebeke et al., 2018; Tanentzap & Monks, 2018, Ritenberga et al, 2018). Therefore, maps of birch pollen emission sources must be developed that reflect the dynamics in birch pollen productivity over space and time. The inter-seasonal variations of vegetation during a long time period can be captured best by remotely-sensed vegetation indices. The Normalized Difference Vegetation Index (NDVI) (Tucker et al., 1979) is a major source on spatio-temporal vegetation presence since a large dataset is available back to the early 1980s (GIMMS NDVI3g, Pinzon & Tucker, 2014).

The main objective of this study is the development of a methodology for building a multi-decadal dataset on birch pollen emission sources which is applied in a pollen transport model SILAM (System for Integrated modeLling of Atmospheric coMposition, http://silam.fmi.fi) (Sofiev et al., 2013, 2015) to reconstruct multi-seasonal airborne birch pollen levels. This methodology is based on merging spaceborne NDVI data with an areal birch tree fraction map derived from forest inventory data (Verstraeten et al., 2019) in a Random Forest statistical framework (Breiman, 2001, Bogawski et al, 2019). This proposed methodology is then evaluated by comparing the daily modelled birch pollen levels near the surface from SILAM driven by ECMWF meteorological data for the period 1982–2019 in a bottom-up approach with long time series of historical pollen observations from aerobiological surveillance networks. Maps with derived temporal trends of the seasonal birch pollen totals (SPIn) are included to demonstrate the potential of this proposed methodology.

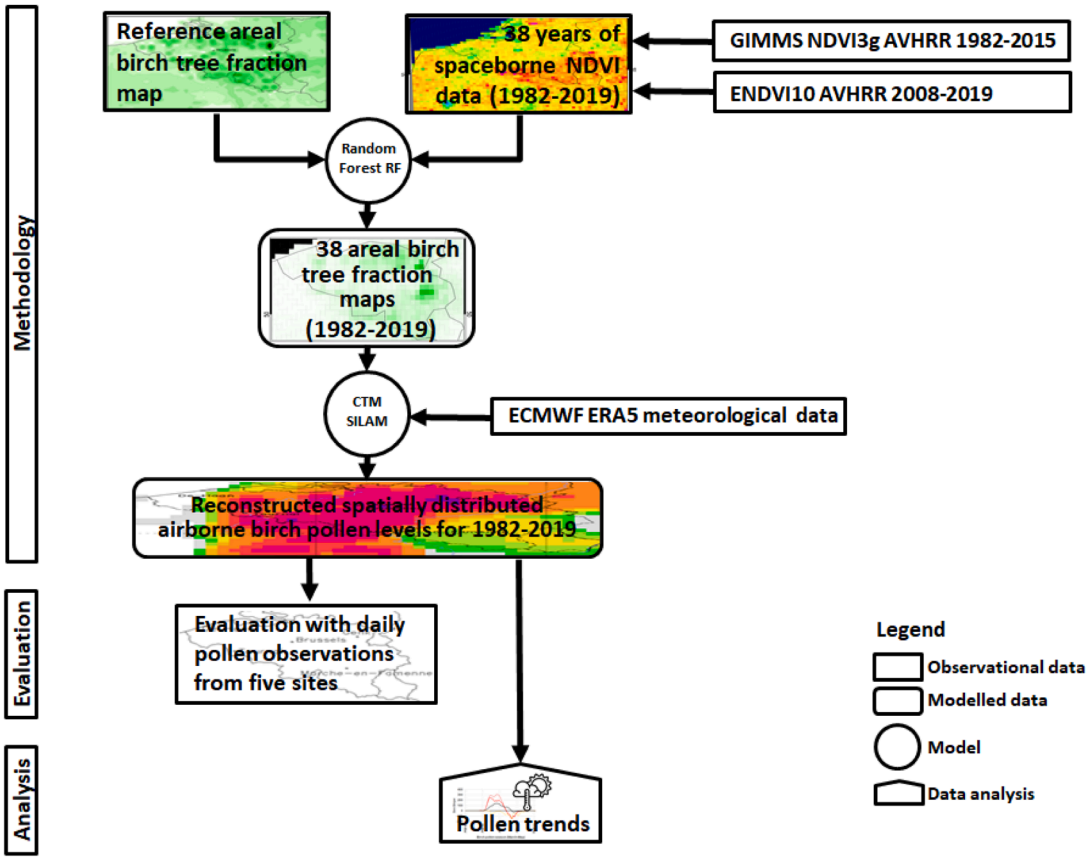

Fig. 1. Schematic overview of the general methodology. Satellite-derived AVHRR/NDVI spanning 1982-2019 are processed. A reference map on areal birch tree fractions is merged with the NDVI time series using Random Forest. These 38 emission maps and the ECMWF meteorological data are input into SILAM to model 38 seasons of airborne birch pollen levels. The methodology is evaluated using daily observed birch pollen levels at five locations. Derived maps are analyzed for long-term trends of pollen levels.

2. Methodology

The general methodology for constructing a multi-decadal dataset on birch pollen emission sources is schematically illustrated in Fig. 1. Overall, a long time series of spaceborne NDVI data is merged with one reference map on areal birch tree fractions using a Random Forest statistical procedure (see Section 2.3 for details) to retrieve a multi-decadal dataset on birch pollen emission sources. The reference birch tree fraction map was derived from local forest inventory data in previous research (Verstraeten et al., 2019). The compiled NDVI data, spanning 1982-2019, was obtained by merging two Advanced Very High Resolution Radiometer (AVHRR) NDVI datasets (see Section 2.2 for details). The GIMMS NDVI3g (Pinzon and Tucker, 2014) dataset covers the period 1982–2015, while the MetOp ENDVI10 dataset covers the period 2008-2019.

The obtained 1982-2019 maps on birch pollen emission sources are used in the SILAM model in a bottom-up approach to simulate 38 years of airborne birch pollen levels near the surface for Belgium at a 0.1° x 0.1° grid using ECMWF meteorological data. We then evaluate the performance of our approach using pollen observations from the Belgian aerobiological surveillance network containing measurements that go back to 1982 (see Section 2.4). Based on our model outputs we then derive maps with temporal trends of the seasonal birch pollen totals (SPIn). Using model scenarios, we can estimate the impact of meteorology and vegetation dynamics on the observed seasonal birch pollen trends covering almost four decades.

2.1. SILAM

The CTM SILAM (System for Integrated modeLling of Atmospheric coMposition, http://silam.fmi.fi) (Sofiev et al., 2013, 2015) is a large-scale dispersion model addressing pollen grains as large biogenic aerosols. SILAM was developed for atmospheric composition and air quality and it includes both Lagrangian and Eulerian advection-diffusion formulations. Here, the Eulerian or box mode is used with a basic horizontal grid cell resolution of 0.1 × 0.1° and a vertical resolution consisting of an uneven distribution of nine layers (thickness of layers from surface to the free troposphere is 25, 50, 100, 200, 400, 750, 1200, 2000, and 2000 m). SILAM integrates the main processes involved in pollen transport such as wind advection, mixing due to turbulence, and dry and wet deposition (Sofiev, 2006; Kouznetsov and Sofiev, 2012; Sofiev et al., 2015). The start and end of the flowering season, which mark the period of the pollen emissions, in SILAM is based on the thermal time flowering model (Sofiev et al., 2006). This start and end are parameterized using temperature sum thresholds (Linkosalo et al., 2010; Sofiev et al., 2013). The major assumption is that the timing of birch flowering is mostly driven by accumulated ambient temperature. The cumulative fraction of pollen released from the start to the end of the pollen season is assumed piecewise linear and proportional to the temperature sum during the main flowering season. Short-term meteorological conditions affect the amount of airborne pollen. Precipitation and humidity inhibit the pollen release from trees, while high wind speed favors the pollen release. Threshold values are used to compute reduction factors from the meteorological data. Typically, the lower and upper thresholds from relative humidity are 50% and 80%, respectively. For precipitation the lower and upper thresholds are 0 and 0.5 mm/h (the grid cell average rate), respectively. At the saturation wind speed of 5 m/s the pollen release rate is maximal. At a wind speed around 1 m/s, no pollen emissions are considered. ECMWF ERA5 reanalysis meteorological data (gridcell of 0.25° x 0.25°) (ECMWF, 2022) is used to drive the transport, emission and deposition of airborne birch pollen in SILAM. SILAM is applied for Belgium for the birch pollen season that in general ranges from March to the end of May for the period 1982–2019, covering almost four decades.

By implementing SILAM we can model the spatial-temporal distributions of airborne birch pollen concentrations near the surface (Verstraeten et al., 2019). Thus, SILAM is a well-established tool for the reconstruction of pollen levels in time. This pollen modelling is based on a bottom-up approach, which means that the spatially distributed pollen emissions sources must be known by SILAM. Hence, maps with the areal fractions of birches are thus crucial underlying datasets. At the European scale, a birch tree fraction map was first compiled and refined by Sofiev et al., (2006) and Sofiev et al., (2013), respectively. In recent previous research we have merged the birch fraction map on the European scale with forest inventory data of birch trees on the scale of Belgium (see for details: Verstraeten et al., 2019) to improve the local birch pollen emissions. This map, with an update with forest inventory data, is used here as reference map (see also the scheme in Fig. 1) for developing multi-decadal datasets on birch pollen emission sources using NDVI data (see next section).

2.2. NDVI data

NDVI (Tucker, 1979) is widely used for monitoring terrestrial vegetation activity and describing vegetation seasonality (Gonsamo et al., 2018). In this study, we have implemented the GIMMS NDVI3g (Pinzon and Tucker, 2014) dataset for the period 1982–2015. This dataset provides bi-monthly NDVI values at a spatial resolution of 1/12° (~8 km). The 3rd generation NDVI is based on the Global Inventory Monitoring and Modeling System (GIMMS) and is assembled from different Advanced Very High Resolution Radiometer (AVHRR) sensors while accounting for various deleterious effects (calibration loss, orbital drift, volcanic eruptions, among others). These AVHRR instruments have provided data from 1981 to the mid-2010s using polar-orbiting meteorological satellites operated by the National Oceanic and Atmospheric Administration (NOAA). Currently, AVHRR sensors are flying on-board the MetOp-A and MetOp-B satellites from EUMETSAT (European Organization for the Exploitation of Meteorological Satellites). In order to extend the NDVI time series to 2019, we also used the 1 km spatial resolution 10-daily composites of the MetOp AVHRR NDVI S10 (ENDVI10, 2021) data. The 10-daily NDVI composites of ENDVI10 are produced from the best available observations in the course of every 10-day period by the orbiting earth observation system MetOp-AVHRR (see also website EUMETSAT, 2021).

For merging both NDVI datasets, we have reprocessed the ENDVI10 data for the period 2008–2019 to the temporal and spatial characteristics of the GIMMS NDVI3g data in three steps. Firstly (i), we have interpolated the 10-daily composites to bi-monthly time steps for each gridcell. Hence, the original 36 time stamps in one complete year are reduced to 24 (twice a month) time stamps. Secondly (ii), we have downscaled the MetOp NDVI data from the original 1 km spatial resolution to the 1/12° grid by spatial averaging in order to match the resolution of the GIMMS $NDVI_{3g}$ grid. In the third step (iii), the overlapping period of both datasets is used for rescaling the MetOp AVHRR NDVI to the NDVI3g dataset for the Region Of Interest (ROI) of Belgium (between 48° and 53°N, and between 1.5° and 7.5°E). For the overlapping period we apply the Savitzky-Golay (Savitzky and Golay 1964) smoothing filter to both NDVI datasets on each gridcell of the ROI. This smoothing filter is based on the convolution process. It fits successive subsets of adjacent data points with a low-degree polynomial using linear least squares. With this filter, short-term fluctuations are smoothed on both time series and the derived bias – the averaged difference - is less affected by high frequency values and the integrated signal is conserved. We then apply the computed bias on the original MetOp AVHRR NDVI to better fit the GIMM $NDVI_{3g}$ dataset. We apply the Savitzky-Golay smoothing filter on the merged datasets. Finally, using the GIMMS NDVI3g and MetOp AVHRR NDVI S10, we have compiled an NDVI dataset that cover the period 1982-2019.

2.3. Seasonal birch pollen emission sources derived from NDVI time series and Random Forest

For modelling airborne birch pollen levels near the surface with SILAM in an emission bottom-up approach, a map with birch pollen emission sources, i.e. a birch tree fraction map, is fundamental model input. At the European scale, such a map was first compiled and refined by Sofiev et al., (2006) and Sofiev et al., (2013), respectively. In previous research, we have merged the birch fraction map on the European scale with forest inventory data of birch trees on the scale of Belgium. This retrieved map is illustrated in Fig. 2 (see for details: Verstraeten et al., 2019). This map was previously applied in modelling birch pollen levels in Belgium (Delcloo et al., 2019; Verstraeten et al., 2019). We refer to this map in this study as the 2008 reference map, since it was implemented for the year 2008 (Verstraeten et al., 2019). The spatial distribution of the areal birch tree fractions is summarized in a boxplot (Fig. 2, inset).

Random Forest is an ensemble decision tree machine learning method (Breiman, 2001; Grange et al., 2018, among others). Briefly (based on Grange and Carslaw, 2019), a single decision tree is formed from a series of binary splits which results in homogeneous groups during a recursive splitting process. Decision trees are non-parametric processes which include interaction and collinearity among variables and which ignore irrelevant variables. Decision trees are fast to train and to make predictions, but they suffer from overfitting. Random Forest controls potential overfitting by sampling (with replacement) the training set with bootstrap aggregation. After training, all the individual tree predictions within the forest are averaged, and this results into a single ensemble model prediction.

We train the Random Forest model using the reference birch tree fraction map for 2008 (derived from local forest inventory data in previous research, Verstraeten et al., 2019), and the corresponding 2008 NDVI data and the latitude and longitude coordinates (derived from the merged GIMMS NDVI3g and the MetOp AVHRR NDVI S10 in Section 2.2). The Random Forest procedure connects the input, i.e. the spatially distributed NDVI data and spatial coordinates to the output, i.e. the 2008 birch fraction map (see also Fig. 2 (a)). Half of the data is used for training and half for testing (Python 3). From this combination, the Random Forest procedure has built a statistical model that converts newly input data (NDVI from other years) to new output data (the corresponding birch tree fraction maps for the other years). As a result, the 1982-2019 NDVI time series and latitude and longitude coordinates are converted in 38 annual maps with birch pollen emission sources. The obtained 38 Model Efficiency values (ME, see also Verstraeten et al., 2006) range between 0.29 and 0.68, with an average value of 0.40.

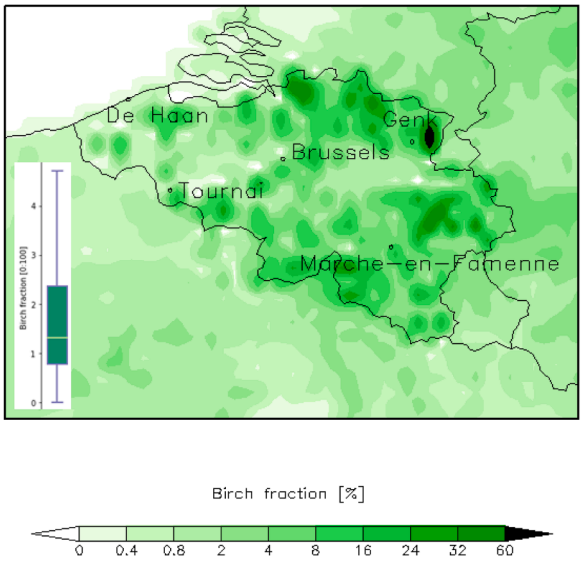

Fig. 2. Spatial distribution of areal birch tree fractions (percentage) in Belgium based on forest inventory data.

2.4. Local pollen observations

The Belgian aerobiological surveillance network (www.airallergy.be) has a longstanding history of observing various types of pollen and fungal spores in the outdoor air since 1982 at the Brussels station, which is one of the oldest and most stable in Europe (Ziello et al, 2012). In total, this network has monitored airborne pollen at 13 different sites. Currently, daily airborne pollen concentrations of 37 tree, shrub and grass taxa are monitored offline at five locations in Belgium (see Fig. 1 and Table 1 for details).

Continuous time series of birch pollen levels for all seasons exists from 1982 on for Brussels and from 1984 on for De Haan. In Tournai seven seasons of daily birch pollen observations are available, and for Genk and Marche-en-Famenne 13 seasons each, but for different years (see Table 1). Pollen observations are performed using a Hirst-type 7-day volumetric spore sampler (Burkard Manufacturing Co., Rickmansworth, UK) (Hirst, 1952). Monitoring complies to the requirements of the European Aerobiology Society (EAS) to the best ability (Galán et al., 2014). Samplers are placed at a height between 10 and 20 m above the ground level. Pollen from various taxa are morphologically identified and manual counted by light microscopy (two longitudinal slide lines reading). The mean daily pollen concentration is then calculated and expressed as pollen grains per cubic meter of air (pollen grains/m^3). Here we used observation datasets encompassing 107 birch pollen seasons from five sites that have been monitored over the period 1982–2019. Not all monitoring sites have been operational during the whole period. Details on the spatial coordinates and the observation periods are included in Table 1. The monitoring stations are also shown in the birch fraction map of Belgium in Fig. 2.

3. Results

3.1. Birch pollen emission source maps based on NDVI

The inter-seasonal differences in the SPIn of birch trees in Belgium is substantial (Coefficient of Variation of 65%, 97%, 65%, 77%, 49% for Brussels, De Haan, Genk, Marche-en-Famenne, Tournai, respectively). In order to add inter-seasonal variability of the maximum amount of birch pollen potentially available for release in the SILAM model, maps with dynamic birch pollen emission sources were reconstructed as input in SILAM. These maps are based on the reference map of areal birch fractions and the NDVI in a Random Forest framework. The relative seasonal variations in the spatial distributions of these maps for Belgium are illustrated in Fig. 3(a). The reference year is 2008 and set to one. We have then normalized the birch tree fraction boxplots for all seasons with respect to the reference season 2008. So, the distributions for the other years are relative to 2008. On average, most birch pollen emission sources are within the 25th and 75th percentage range of the neighboring years (between 2nd and 4th quartile) given the 1982–2019 period. The average values vary between ~ 0.75 and ~1.30 with respect to 2008.

Table 1
The location of the pollen monitoring stations of the Belgian aerobiological surveillance network and the corresponding observation periods available for this study. In total, 107 birch pollen seasons (1st March-30th June) were included.

Pollen monitoring locations	Latitude / Longitude	Period
De Haan	51.274 N / 3.022 E	1984–2019
Tournai	50.614 N / 3.387 E	2013–2019
Brussels	50.825 N / 4.383 E	1982–2019
Marche-en-Famenne	50.200 N / 5.312 E	2001–2005 and 2012-2019
Genk	50.965 N / 5.495 E	2001–2004 and 2011–2019

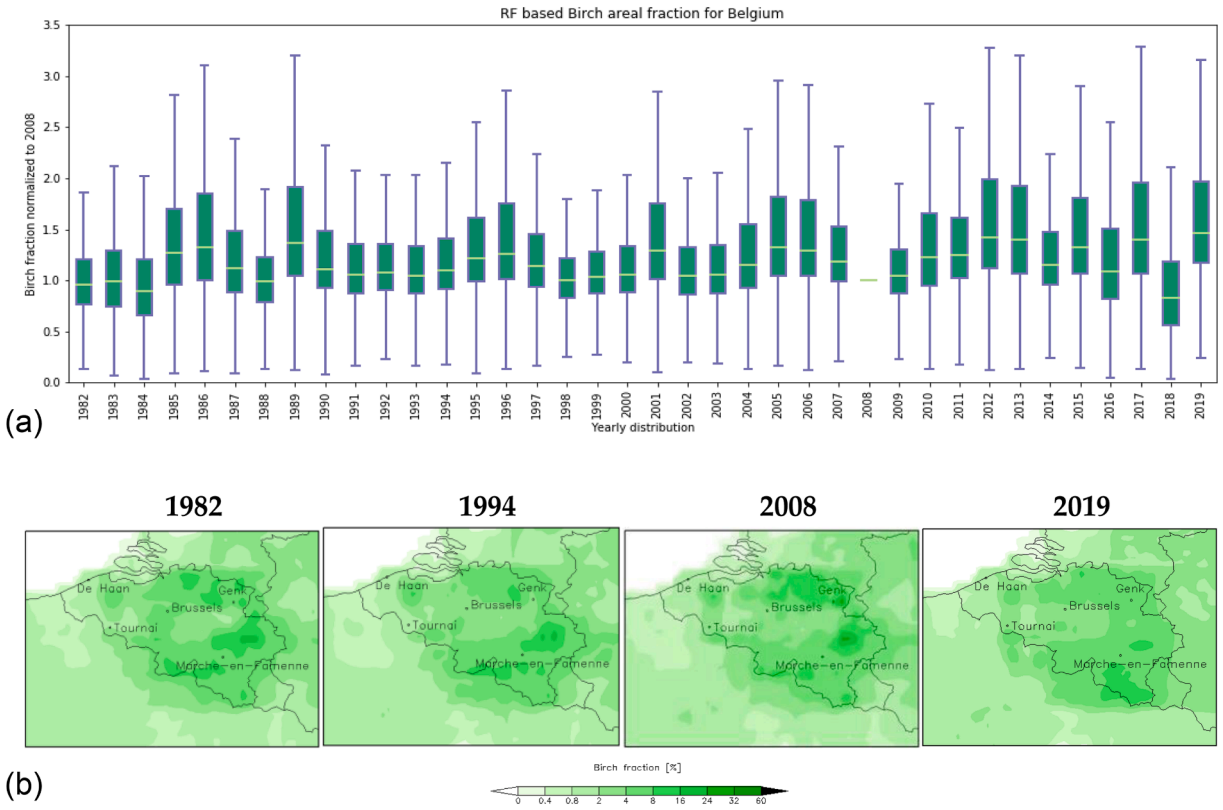

Fig. 3. (a) The relative variations in the distributions of birch pollen emissions sources in Belgium for the period 1982-2019 with respect to 2008 (set to one, normalization) using the Random Forest statistical approach on the GIMMS/MetOp NDVI time series and the areal birch fraction map of Fig. 2 as reference. The boxplot of the reference map for 2008 with the spatial distribution of the actual birch tree fractions is shown in Fig. 2 and is set to one. (b) Illustrations of 1982, 1994, 2008, 2019 birch tree fractions maps derived from NDVI and RF.

The 25^{th} - 75^{th} range can be both small (i.e. 1982, 1998) as well as large (i.e. 1989, 2017). To illustrate the obtained output of the Random Forest framework and NDVI data, birch tree fraction maps for some seasons are shown in Fig. 3 (b).

The largest deviation from 2008 is in 2018, showing the lowest values in birch pollen emission sources. In the last decade, the variations seem higher (larger 25^{th} - 75^{th} ranges between birch seasons). The low and high extreme values are also larger compared to the period 1982-2007. For Brussels, the birch pollen emission sources value is on average 0.53, and varies between 0.14 and 1.46 for the 1982-2019 period as extracted from the gridcell containing Brussels of the 38 maps of birch pollen emission sources. These 38 maps are used as input in SILAM for modelling the 1982-2019 spatially distributed birch pollen levels near the surface for Belgium. Since vegetation activity as derived from spaceborne vegetation indices or Gross Primary Productivity (GPP, or plant photosynthesis) lags behind some seasons on the SPIn, we have introduced a 2-year shift in the NDVI-based emission sources used in SILAM in agreement with Verstraeten et al., (2019). So, the 1982 NDVI based birch pollen emission source is used in the 1984 SILAM run, 1983 NDVI for the 1985 SILAM run and so on.

3.2. *Time series of modelled and observed airborne birch pollen levels*

SILAM was run for the period 1982–2019 using ERA5 ECMWF meteorological data for two scenarios. In the reference (REF) scenario (i), the 2008 areal birch fraction map was used to model the daily birch pollen levels for all birch seasons from 1982 to 2019. In the updated (UPD) scenario (ii) SILAM was run using the 38 seasons of birch emission sources based on the 1982-2019 NDVI time series and the 2008 reference map of areal birch fractions in a Random Forest approach, shifted forward by two years. Airborne birch pollen levels near the surface at daily basis for the period 1982-2019 were extracted from the SILAM output for each pollen monitoring station from Fig. 2 and compared with observations. As an illustration, the complete time series are shown for Brussels and De Haan in Fig. 4 (two stations with the longest observation history).

As illustrated in Fig. 4, the updated run of SILAM for Brussels generally reduces the amount of birch pollen grains in the air. This is shown by the negative difference between the UPD and REF run on the right y-axis of Fig. 4. For De Haan, however, the updated SILAM run increases the birch pollen amounts. In order to evaluate the model performance for the individual birch seasons at all the five available monitoring stations, the determination coefficients (R^2) and the slopes between the observed and modelled daily birch pollen levels are plotted in Fig. 5 spanning the period 1982–2019 into Taylor diagrams for three birch pollen emission source maps.

Taylor diagrams (Taylor, 2001) can graphically illustrate the behavior or performances of models at different time periods (pollen seasons for example) described in terms of three statistical measures. Here we use only two statistical measures (R^2 values and slopes between the observed and modelled daily birch pollen levels). Optimally, all seasons should be close to the dashed arc (slope is one) and close to an R^2 value of one. This location is indicated as a star (*) in the diagrams of Fig. 5. The Taylor diagram (Fig. 5) for Brussels shows a cluster of seasons between R^2 values of 0.30 and 0.80 with slopes (modelled vs observed daily values) ranging from ~0.40 to 1.35. For De Haan, however, most R^2 values are smaller than 0.60, with slopes that vary between 0.20 and 1.40. For Genk, all R^2 values are more clustered between ~0.50 and 0.80 with slopes that show a large spread. The R^2 and slope values for Marche-en-Famenne are very scattered, while for Tournai the scatter is much smaller. So in general, plenty of birch pollen seasons show reasonably high R^2 values, especially for the monitoring sites of Brussels,

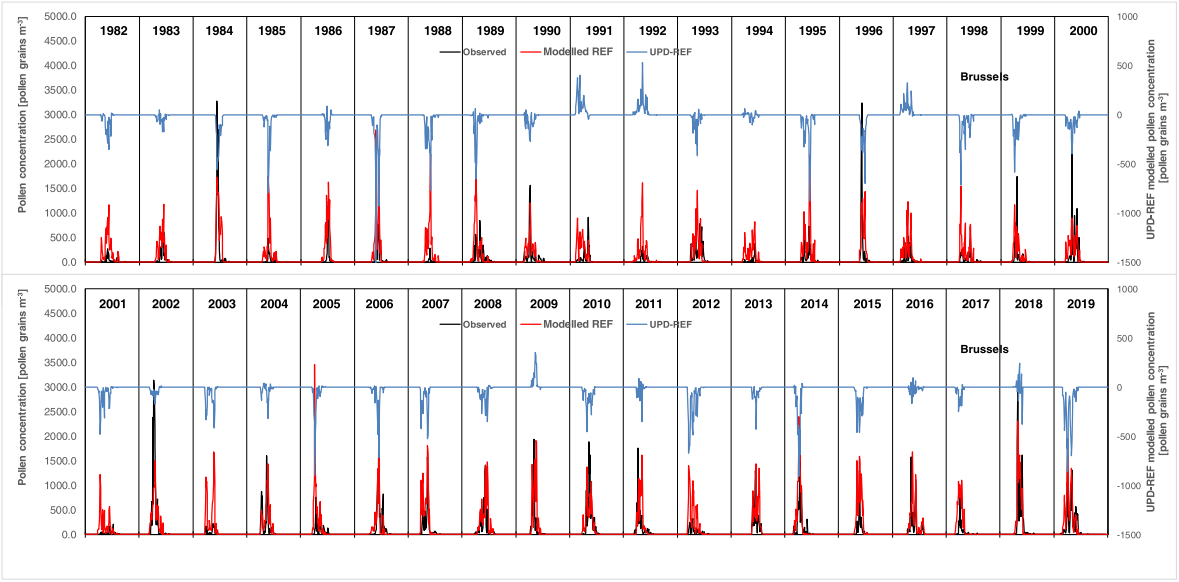

(a)

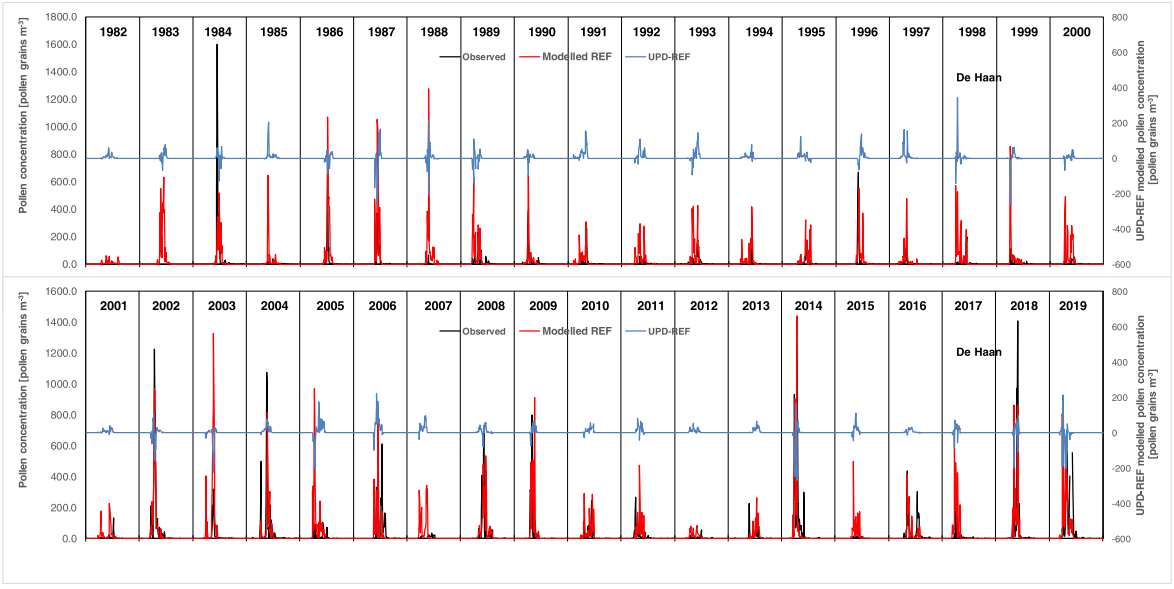

(b)

Fig. 4. The observed (black) and modelled (reference run in red) 1982-2019 daily airborne birch pollen level time series near the surface (pollen grains m^{-3}) at the monitoring stations of Brussels (a) (two upper panels, range 1982-2000 and 2001-2019) and De Haan (b) (two lower panels). In blue the contribution of the variable birch pollen emission sources to the airborne pollen levels of the updated model run by taking the difference between the updated (UPD) and reference (REF) SILAM run.

Genk, Marche-en-Famenne and Tournai (see Fig. 5, Taylor diagrams and time series). Some seasons, however, show bad model performance (1991, 2001, 2005 for Brussels). The 1982-2019 overall R^2 values for these monitoring stations are 0.27, 0.36, 0.53, 0.46 and 0.56, respectively (see Table 2). This table shows the slope, intercept and determination coefficients (R^2) between the daily observed and modelled birch pollen levels for the period 1982-2019 (not individual seasons) at all the monitoring stations available for this study.

The 1982-2019 R^2 values for the monitoring station of De Haan are in general much lower (overall 0.27 for the NDVI case, Table 2) than for the other sites (up to 0.58). This station is located at the vicinity of the North Sea. Very low values ($R^2 < 0.10$) are observed in 1998, 2001, 2005-2007, 2012. The monitoring station of Marche-en-Famenne performs well for the NDVI based update, except for 2002. The mean R^2 values (for the separate seasons, NDVI based) are 0.34, 0.51, 0.62, 0.56, and 0.63 for De Haan, Brussels, Genk, Marche-en-Famenne and Tournai, respectively. The critical threshold above which the majority of sensitized patients is considered to develop allergy symptoms is under debate (Steckling-Muschack et al., 2021). The Belgian aerobiological surveillance network uses so far the daily 80 birch pollen grains/m^3 as indicatory threshold value. Based on the dichotomous classification using Odds Ratio (OR) (Siljamo et al., 2013; Ritenberga et al., 2018), SILAM is able to detect pollen levels larger than this threshold with OR values between 10 and 21 at the five monitoring sites. The OR values are also larger than 8 for the thresholds of 25 or 50 birch pollen grains/m^3. OR is a statistic that quantifies the strength of the association between two events. If the ratio is one, both events are not associated to each other. If the OR is larger or smaller than one, then there is a positive or negative association, respectively. Here the OR is computed as the ratio of the probability of detection of correct high predictions and the probability of false detection giving low-concentration that are predicted as high. More explanation on the used formulas are provided in Siljamo et al., (2013).

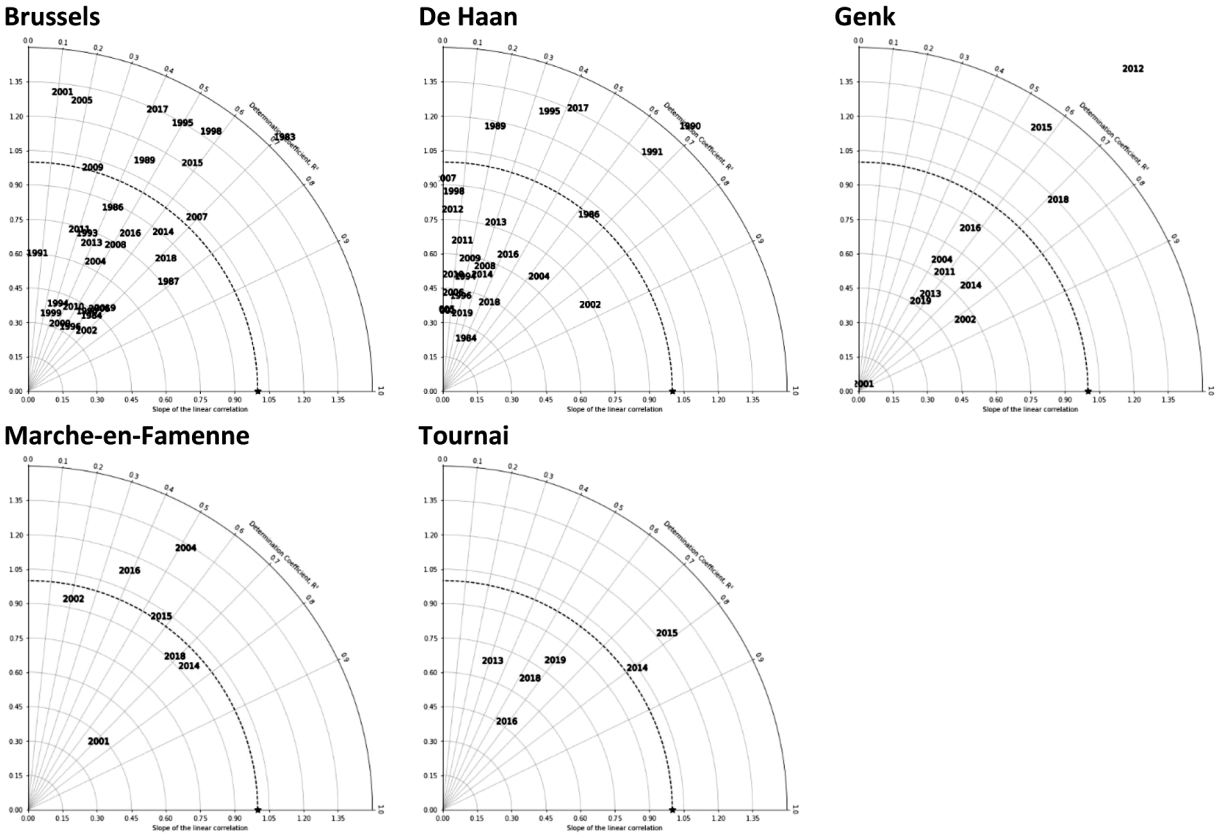

Fig. 5. Taylor diagrams including the determination coefficient (R^2) and the slopes between the daily SILAM-modelled and observed birch pollen concentrations for each pollen season from 1982 to 2019 at five pollen monitoring stations in Belgium (107 birch seasons).

Table 2
Slope, intercept and the determination coefficient (R^2) between the daily observed and SILAM modelled birch pollen levels at five pollen monitoring stations in Belgium (107 seasons) covering the period 1982–2019.

	Daily Values	De Haan	Brussels	Genk	Marche-en-Famenne	Tournai
UPDATE NDVI RF	Slope	0.70	0.61	0.75	0.12	0.78
	Intercept	22.32	47.74	55.22	73.84	21.76
	R^2	0.27	0.36	0.53	0.46	0.56

3.3. Analyzing four decades of reconstructed birch pollen levels

In order to explore the behavior of the birch pollen over time, we have computed the change rate in seasonal birch pollen cycles based on daily pollen levels. We apply the methodology as described in Bruffaerts et al., (2018) for the observations and modelled data of Brussels (i.e. longest time series). It is based on computing Sen slopes from mean daily pollen concentration data, considering different years of a given calendar day. This is a method for robustly fitting a line to sample points in the plane (simple linear regression) by choosing the median of the slopes of all lines through pairs of points (Theil, 1950; Sen 1968). It is based on non-parametric statistics and the estimator is insensitive to outliers. Briefly, in this method the Sen slope values are computed for each day of the pollen season for the period 1982-2019 (Makra et al., 2011). The obtained curve with Sen slopes for each day of the pollen season was then smoothed with the LOcally Estimated Scatterplot Smoothing (LOESS) method (García-Mozo et al., 2014), setting the span to 0.1. As an indicator for overall trend, the Area Under the Curve (AUC) was calculated by the trapezoidal method. This methodology is very appropriate for the analysis of local changes in pollen levels and has the advantage to illustrate changes that occur within the pollen season including shifts in the start and end of the season. In Fig. 6, the change rate is shown of the seasonal cycles of daily birch pollen levels between 1982 and 2019 as observed at the monitoring station of Brussels (in black line), and as modelled by SILAM using the 38 maps of birch pollen emission sources based on NDVI and RF (UPD in red line), and using only one reference map for the period 1982-2019 (REF, dashed brown). The change rate is computed for the difference of the UPD and REF SILAM run time series (see dashed yellow). Fig. 6 illustrates these curves applied for the airborne birch pollen observations in Brussels for

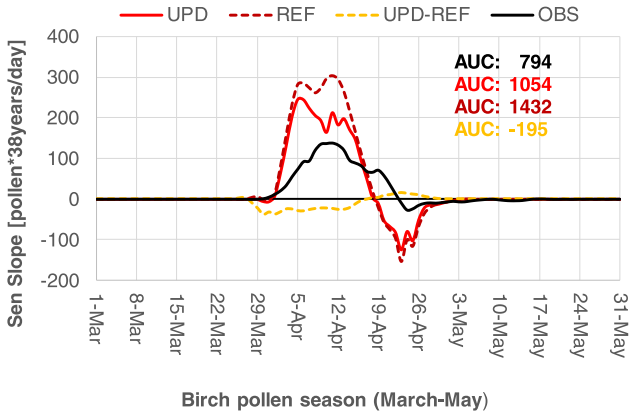

Fig. 6. Change rate in the seasonal cycles of daily birch pollen levels between 1982 and 2019 as observed at the monitoring station of Brussels (in black line), and as modelled by SILAM using the 38 maps of birch pollen emission sources based on NDVI and RF (UPD in red line), as using only one reference map for the period 1982-2019 (REF, dashed brown), and the difference (see dashed yellow). The area under the curve (AUC) is included.

1982-2019 and the corresponding levels using the REF and UPD SILAM. The AUC values are in the same order of magnitude for the observations (794) and the UPD model run (1054), indicating comparable temporal behavior of the birch seasons over four decades. For the REF run, however, the AUC is substantially higher (1432). Apart from similarities, also differences in the seasonal cycle between observations and model runs can be derived from Fig. 6. Between the end of March and mid-April, the curves are more comparable. The model values show negative trends for the 3rd week of April on, while the trends in the observations lag behind by 4 days. The slopes in the early and late period of the birch pollen season are much steeper (increasing and decreasing, respectively) for the models compared with the slopes computed from the observations. The slopes of the UPD run and observations are more similar in the middle part of the birch pollen season. More complicated is that the AUC value computed from the daily slopes based on the difference of the UPD and REF SILAM runs (AUC = -195) is not just the difference of the AUC values separately computed from the UPD and REF SILAM runs (AUC = -378). By taking the difference between the UPD and REF SILAM runs (UPD-REF), we can isolate the contribution of the changing birch pollen emission sources over 1982-2019 to the changing amount of pollen in the air driven by meteorology. The difference in the daily slopes of the birch pollen season computed for the UPD and REF runs separately deviates strongly from the daily slopes directly computed from the difference of the UPD and REF runs.

Large (absolute) effect of the dynamic birch pollen emission sources is observed in early April (from 6th on for Brussels) until 14-16 April. Then it is close to zero during 17-19th April which is roughly after the peak of the birch pollen season in Belgium. During the period 20-30th April, more towards the end of the season, it is high again with the highest (absolute values) impact on 23rd April. Finally, in the end tail of the season it turns close to zero again, indicating almost no effect of the variable birch pollen emission sources. During the middle part of the pollen season (e.g. peaks), the zero impact suggests that the increase of airborne pollen levels is primarily driven by meteorology and hence climate variations. The negative peak values during the early and mid-stage and the late stage of the pollen season might imply that the variations in pollen sources (birch trees) dampen the positive change rate of the amount of pollen in the air during this stages of the season induced by meteorological variations and climate effects. Stated otherwise, the dynamic birch pollen emission sources clearly reduce the climate

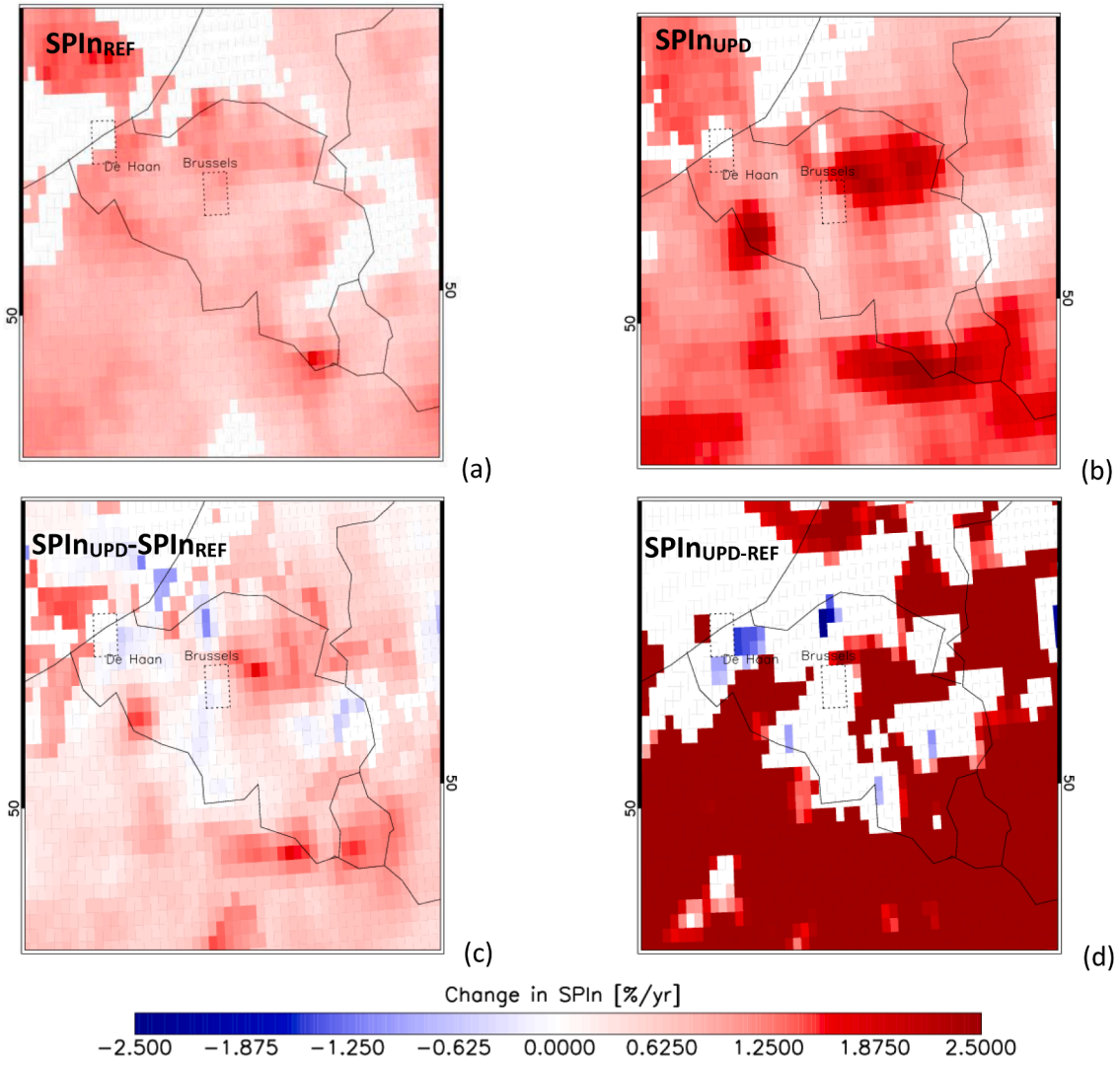

Fig. 7. Spatial distribution of the temporal change rate represented by the smoothed Seasonal Pollen Integral (SPIn) of airborne birch pollen levels in Belgium derived from SILAM runs for the period 1982-2019 (maps made in IDL.8.5.1). (a) Change in SPIn for the reference (REF) SILAM run solely reflecting the variable meteorology (**SPIn$_{REF}$**). (b) Change in SPIn for the updated (UPD) SILAM model run showing the combined effect of variations in meteorology and in birch pollen emission sources based on the NDVI (**SPIn$_{UPD}$**). (c) The difference of the changes in SPIn values of maps (b) and (a) (**SPIn$_{UPD}$-SPIn$_{REF}$**). (d) Change in SPIn values computed for the difference of the updated and reference SILAM model run (**SPIn$_{UPD-REF}$**). Only statistically significant Sen slope values are shown ($P < 0.05$).

impacts on increases in airborne birch pollen levels in the SILAM model run with at least ~-14% (-195/1432×100) for the gridcell and site in Brussels. This corresponds with ~3.6% per decade. Considering the AUC_{UPD} of 1054 and the AUC_{REF} of 1432, the change per decade is ~-7.0% computed as (1054-1432)/1432×100.

In order to illustrate the spatial distribution of seasonal pollen level trends for birches during the period 1982-2019 over Belgium based on SILAM, we compute the Sen slopes on the smoothed SPIn for the REF and UPD SILAM model runs as shown in Fig. 7. The Boxcar filter with a span of three years was applied to smooth for masting cycles (Hoebeke et al., 2018). The rectangular areas on the maps illustrate the different pollen levels in neighboring gridcells close to the monitoring stations of Brussels and De Haan. Time series analysis based on SPIn values is more traditional than using the AUC values from daily pollen cycle values. Fig. 7 shows that the REF SILAM run produces in general higher trends than the UPD run (Fig. 7(a),(b)), which is similar as observed in Fig. 6 for the daily values of Brussels (AUC).

The trends of the SPIn of the UPD run compared to REF values illustrate a mixed pattern (see difference map in Fig. 7(c)). Most areas in Belgium show an increase, although four smaller parts with decreasing trends can be distinguished (in the west, north, south-west and east). The SPIn trend values computed on the difference of the UPD and REF SILAM runs (UPD-REF, Fig. 7(d)) are mainly insignificant (white color in the maps indicating P-values ≥ 0.05) or positive (red color), with locally some negative trend values in areas with substantial birch trees as suggested in the map of Fig. 7(a) (REF SILAM run) and the fraction map of Fig. 1. The gridcells with negative values for the UPD-REF scenario (Fig. 7(d)) imply a decelerating effect or slow-down on the increasing pollen levels in the air due to the dynamics and change in the pollen emission sources between seasons. The positive values for the UPD-REF scenario (Fig. 7(d)), however, suggest an accelerating impact of the pollen emission source dynamics on the airborne pollen levels.

Overall for Belgium, an increase of 8.2%/decade in the amount of airborne birch pollen is observed from the SILAM run based on the REF birch fraction map. Based on the UPD run of SILAM using NDVI in a RF methodology to produce 38 maps with birch pollen emission sources, an increase in birch pollen grains of 13.1%/decade is observed. This is much higher compared to the REF run (+4.9%/decade). It indicates an accelerating or intensifying effect in the seasonal birch pollen increase with 59.8% per decade (+4.9/8.2×100) when vegetation dynamics are included in the model. This contrasts with the AUC based value of -7.0%/decade reported for Brussels (Fig. 6), but agrees well with the general increasing trend in birch pollen emission sources in Belgium as shown in Fig. 8. For Brussels, indeed, the slope is negative (blue values) resulting in a more moderate increase of airborne birch pollen levels since only meteorological induced increasing effects play. The significant gridcells for Brussels (blue values) correspond to decadal decreases in birch pollen emissions sources between ~ -6.4 and -9.4%.

4. Discussions

The birch pollen emission sources ingested by SILAM were updated based on a bottom-up approach, so no model parameters on pollen release must be changed (Prank et al., 2013; Verstraeten et al., 2019, 2021). The NDVI was used for introducing seasonal dynamics to the pollen emission sources since this index is associated to vegetation cover and implemented in pollen research (Khwarahma et al., 2017; González-Naharro at al., 2019). We have applied the Random Forest approach on the NDVI data and the reference birch fraction map based on forest inventory data since this and similar methods have been demonstrated to give promising results in airborne pollen research (Bogawski et al., 2019; González-Naharro at al., 2019). The obtained 1982–2019 birch pollen emission source maps reflect the inter-seasonal dynamics of the SPIn, the pollen productivity, rather than variations in real areal birch fractions. These maps are apparent areal birch fraction maps since we cannot assume that the amount of birch trees changes that quickly. That is why we refer to these maps as birch pollen emission source maps. These fraction maps form the basic input into SILAM to quantify the distribution of the birch pollen emission sources which is related to the year-to-year changes in the SPIn. As before mentioned, vegetation activity lags behind some seasons on the SPIn (Hoebeke et al., 2018, Ritenberga et al., 2018), so we have introduced a 2-year shift in the NDVI-based emission sources as previously done (Verstraeten et al., 2019). The correlation (R^2) between the birch fractions based on NDVI and the SPIn monitored at Brussels is 0.10, only if a shift of two years is introduced, otherwise it is close to zero.

Over almost four decades, the SILAM model performed well with R^2 values up to 0.56, and higher values for individual seasons (Fig. 3, Table 2). This is in agreement with results reported by Siljamo et al., (2013) for several stations, with Sofiev et al., (2015) for multi-model comparison, and Ritenberga et al., (2016) for Riga. The model performance also depends on the quality of the observed pollen data derived from the Hirst observation method which is also subjected to uncertainty (Oteros et al, 2017, Rojo et al., 2019). What is more, the reference data might differ from other methods since for instance a portable sampler to monitor pollen at street level reported birch pollen ~10 days earlier

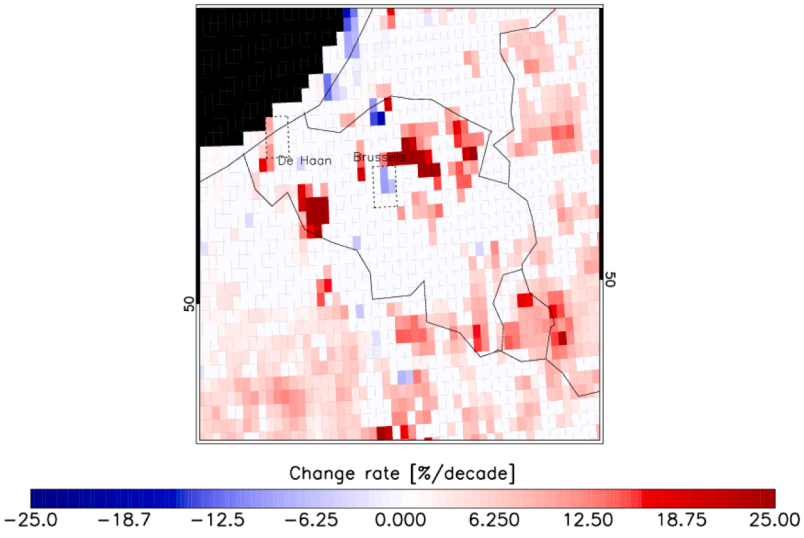

Fig. 8. Spatial distribution of the temporal change rate in birch pollen emission sources in Belgium derived from the 1982-2019 birch pollen emission source maps based on NDVI time series and Random Forest. Only statistically significant slope values are shown ($P< 0.05$).

than at the rooftop level (de Weger et al., 2020).

The change rate in seasonal birch pollen cycles based on daily pollen levels for the period 1982–2019 shows substantial increases. This was associated to the temperature rise over four decades, as suggested by the observed temperature anomaly trend of 0.4 °C per decade at the meteorological station of Ukkel in Brussels (period 1981-2020, KMI, 2021) and other studies. For observations back to 1977, de Weger et al., (2021) also suggest these climate effects for the BENELUX (Belgium, the Netherlands, Luxemburg) on birch pollen releases. Anderegg et al., (2021) have reported increases in pollen concentrations across North America over the last three decades, which are strongly coupled to observed warming. Tree pollen showed the largest increases in spring and SPIn values. Ziska et al., (2019) have studied the northern hemisphere in a retrospective data analysis (including observation data in Belgium) and found that ongoing increases in temperature extremes (T_{min} and T_{max}) might already be contributing to higher pollen load for multiple allergenic pollen taxa. Also for the Mediterranean tree taxa, larger pollen quantities were found to be emitted to the atmosphere (Fernández-Llamazares et al., 2014). In Ireland, airborne birch pollen concentrations have risen over the last 40 years, which was related to increases in the fraction of birch trees in forest areas as well as ornamental use (Maya-Manzano et al., 2021).

The effect of the variable birch pollen emission sources on the change rate of the birch pollen seasonal cycle (Fig. 6) and on the SPIn (Fig. 7) suggests a mix of dampening and amplification on the amount of emitted pollen associated to the temperature increases of the last four decades by birches. The intensified rise of birch pollen levels corresponds to increases of the birch pollen emissions sources over 38 years in large parts of Belgium as demonstrated in Fig. 8. This is in line with an Irish study (Maya-Manzano et al., 2021) that associates the higher amount of birch pollen over time to the increased fraction of birch trees. The question how models will cope with airborne pollen levels when more detailed (high resolution) emission maps are introduced over such a long period as done in this study must be investigated further.

The results of the model-measurement comparison also contribute to the on-going discussion on whether the European vegetation already started accommodating to the warmer temperatures. In particular Fu et al., (2015), based on phenological data collected in Germany, argued for a very substantial reduction of thermal sensitivity of the majority of the European trees. For birch, the suggested reduction of the sensitivity is as large as 1.3 – 2.0 days/°C of difference between 1980–1999 and 2000–2013 periods. So strong adaptation effect would render all models performing well in 1980s inadequate in 2010s. However, we did not see such trend: the same thermal sensitivity was applied in SILAM throughout the whole period with no significant trend in the model performance.

5. Conclusions and future research

A methodology was developed to reconstruct multi-decadal airborne birch pollen levels near the surface using the SILAM chemistry transport model in a bottom-up emission approach of birch pollen sources for Belgium. This methodology consisted of the combination of a birch fraction map derived from the forest inventory data from previous research with 38 years of AVHRR-GIMMS3g NDVI data (1982–2015) extended with NDVI data from MetOp-AVHRR after 2015 using a Random Forest statistical approach. Daily observation data of five birch pollen monitoring stations were used to evaluate the simulated airborne birch pollen levels. The mean R^2 values of individual pollen seasons between daily observed and SILAM modelled birch pollen levels range from 0.35 to 0.63, but for individual seasons the value can go up to 0.86. The overall R^2 values at the monitoring sites, combining all the 1982-2019 seasons where available, range from 0.27 to 0.56. This is an indication of the good performance of SILAM for Belgium. Temporal analysis of daily airborne pollen data shows a substantial increase of the amount of pollen emitted over time, evident both from the observations in Brussels as well as from the SILAM run with the updated emission inventory. On average, for Belgium there is an increase of 13.1% per decade. SILAM model results suggest an enhanced effect of almost 4.9% per decade on the amount of emitted pollen. Hence, the increase in levels of airborne birch pollen over time is mainly climate-induced (8.2% per decade), but it is amplified by the increase in the emission sources.

The impact of climate change on the dynamics of long-range transport of birch pollen levels can be substantial and should be investigated in more details. Application of NDVI as a proxy of lagged pollen production showed its potential, but integration of available remotely-sensed vegetation indices at higher resolutions for Belgium and beyond in future research should be of great interest to increase the detail of the birch pollen emission source maps. Implementing the developed methodology to use the NDVI and birch fraction maps in a statistical framework for running SILAM on the European scale and other continents in combination with long time series of pollen observations can be of great benefit to improve our understanding in birch pollen induced air allergies. Improving pollen dispersion models by the incorporation of observed pollen data in the model emission sources should be further investigated, including the possibilities of the assimilation of near-real-time observed pollen data in CTMs. Finally, the next step is to set-up and test the SILAM model in a birch pollen forecasting mode for Belgium.

Funding

This research was partly funded by the Belgian Science Policy Office (BELSPO) in the frame of the Belgian Research Action through Interdisciplinary Networks Brain (BRAIN.be) programme – project RETROPOLLEN (B2/191/P2/RETROPOLLEN) and partly funded by the Royal Meteorological Institute of Belgium. The SILAM general development has been funded by the Academy of Finland project PS4A (grant 318194).

CRediT authorship contribution statement

Willem W. Verstraeten: Conceptualization, Methodology, Software, Validation, Formal analysis, Investigation, Resources, Data curation, Writing – original draft, Visualization, Project administration, Funding acquisition. **Rostislav Kouznetsov:** Software, Resources, Writing – review & editing. **Lucie Hoebeke:** Validation, Data curation, Writing – review & editing. **Nicolas Bruffaerts:** Validation, Resources, Data curation, Writing – review & editing, Project administration, Funding acquisition. **Mikhail Sofiev:** Software, Resources, Writing – review & editing. **Andy W. Delcloo:** Software, Resources, Data curation, Writing – review & editing, Project administration, Funding acquisition.

Declaration of Competing Interest

The authors declare no conflict of interest. The funders had no role in the design of the study; in the collection, analyses, or interpretation of data; in the writing of the manuscript, or in the decision to publish the results.

References

Anderegg, W.R.L., Abatzoglou, J.T., Anderegg, L.D.L, Bielory, L., Kinney, P.L., Ziskai, L., 2021. Anthropogenic climate change is worsening North American pollen seasons. PNAS 118. https://doi.org/10.1073/pnas.2013284118, 2021.

Baldacci, S, Maio, S., Angino, A. et al., 2018. *European Respiratory Journal*2018 52: PA1151; DOI: 10.1183/13993003.congress-2018.PA1151.

Beggs, P.J., 2004. Impacts of climate change on aeroallergens: past and future. Clin. Exp. Allergy 34, 1507–1513.

Beggs, P.J., 2021. Climate change, aeroallergens, and the aeroexposome. Environ. Res. Lett. 16, 035006.

Bieber, T. et al., 2016. Global Allergy Forum and 3rd Davos Declaration 2015: Atopic dermatitis/Eczema: Challenges and opportunities toward precision medicine. *Allergy* 71, 588–592.
Blomme, K., Tomassen, P., Lapeere, H., et al., 2013. Prevalence of allergic sensitization versus allergic rhinitis symptoms in an unselected population. International Archives of Allergy and Immunology 160 (2), 200–207.
Bogawski, P., Grewling, L., Jackowiak, B., 2019. Predicting the onset of Betula pendula flowering in Poznań (Poland) using remote sensing thermal data. Science of the Total Environment 658, 1485–1499, 2019.
Bousquet, J., Anto, J.M., Bachert, C. et al., 2020. Allergic rhinitis. *Nat Rev Dis Primers*6, 95. https://doi.org/10.1038/s41572-020-00227-0.
Breiman, L., 2001. Random Forests. Machine Learning 45, 5–32, 2001.
Bruffaerts, N., De Smedt, T., Delcloo, A., Simons, K., Hoebeke, L, et al., 2018. Comparative long-term trend analysis of daily weather conditions with daily pollen concentrations in Brussels, Belgium. Int. J. Biometeorol. 62 (3), 483–491. https://doi.org/10.1007/s00484-017-1457-3.
Clement, J., Maes, P., van Ypersele de Strihou, Ch., van der Groen, G., Barrios, J.M., Verstraeten, W.W., van Ranst, M., 2010. Beechnuts and outbreaks of nephropathia epidemica (NE): of mast, mice and men. Nephrol. Dial Transplant 25, 1740–1746. https://doi.org/10.1093/ndt/gfq122.
D'Amato, G, Cecchi, L, Bonini, S, et al., 2007. Allergenic pollen and pollen allergy in Europe. Allergy 62, 976–990. https://doi.org/10.1111/j.1398-9995.2007.01393.x.
Delcloo, A., Verstraeten, W.W., Dujardin, S. et al., 2019. Spatio-Temporal Monitoring and Modelling of Birch Pollen in Belgium. Air Pollution Modeling and its Application XXVI. DOI 10.1007/978-3-030-22055-6_12.
de Weger, L.A., Molster, F., de Raat, K., et al., 2020. A new portable sampler to monitor pollen at street level in the environment of patients. Sci. Total Environ. 741, 140404.
de Weger, L.A., Bruffaerts, N., Koenders, M.M.J.F., et al., 2021. Long-term pollen monitoring in the Benelux: Evaluation of allergenic pollen levels and temporal variations of pollen seasons. Front. Allergy 2 (30). https://doi.org/10.3389/falgy.2021.676176.
ECMWF, https://www.ecmwf.int/en/newsletter/147/news/era5-reanalysis-production. 2022.
ENDVI10, 2021. Normalized Difference Vegetation Index, PRODUCTS: LSA-420 AND LSA-454 (ENDVI10). SAF/LAND/VITO/PUM_ENDVI10v2Issue/Revision Index: Issue 3. Last Change:21/01/2021. https://nextcloud.lsasvcs.ipma.pt/s/tmDP8S5HomDSPd4?dir=undefinedandopenfile=136004 (accessed on 10 March 2021).
EUMETSAT, https://navigator.eumetsat.int/product/EO:EUM:DAT:METOP:ENDVI10 (accessed on 9 December 2021).
EEA, European Environment Agency, 2017. Air pollution sources. https://www.eea.europa.eu/themes/air/air-pollution-sources-1. Access 6 April 2020.
Fernández-Llamazares, A., Belmonte, J., Delgado, R., De Linares, C., 2014. A statistical approach to bioclimatic trend detection in the airborne pollen records of Catalonia (NE Spain). Int. J. Biometeorol. 58, 371–382. https://doi.org/10.1007/s00484-013-0632-4. *2014*.
Fu, Y.H., Zhao, H., Piao, S., Peaucelle, M., Peng, S., Zhou, G., Ciais, P., Huang, M., Menzel, A., Peñuelas, J., Song, Y., Vitasse, Y., Zeng, Z., Janssens, I.A., 2015. Declining global warming effects on the phenology of spring leaf unfolding. Nature 526, 104–107. https://doi.org/10.1038/nature15402.
Galán, C., Smith, M., Thibaudon, M., et al., 2014. Pollen monitoring: minimum requirements and reproducibility of analysis. Aerobiologia. https://doi.org/10.1007/s10453-014-9335-5, 30, 385.
Galán, C., Ariatti, A., Bonini, M., et al., 2017. Recommended terminology for aerobiological studies. Aerobiologia 33, 293–295. https://doi.org/10.1007/s10453-017-9496-0, 2017.
Gonsamo, A., Chen, J.M., Ooi, Y.W., 2018. Peak season plant activity shift towards spring is reflected by increasing carbon uptake by extratropical ecosystems. Glob. Chang. Biol. 24, 2117–2128.
González-Naharro, R, Quirós, E., Fernández-Rodríguez, S., et al., 2019. Relationship of NDVI and oak (Quercus) pollen including a predictive model in the SW Mediterranean region. Sci. Total Environ. 676, 407–419, 2019.
García-Mozo, H., Yaezel, L., Oteros, J., Galán, C., 2014. Statistical approach to the analysis of olive long-term pollen season trends in southern Spain. Sci. Total Environ. 473-474, 103–109.
Grange, S.K., Carslaw, D.C., Lewis, A.C., Boleti, E., Hueglin, C., 2018. Random forest meteorological normalisation models for SwissPM10 trend analysis. May. Atmos. Chem. Phys. 18 (9), 6223–6239. https://www.atmos-chem-phys.net/18/6223/2018/.
Grange, S.K., Carslox, D.C., 2019. Using meteorological normalisation to detect interventions in air quality time series. Sci. Total Environ. 653 https://doi.org/10.1016/j.scitotenv (2019) 578–5882018.10.344.
Hirst, J.M, 1952. An Automatic Volumetric Spore Trap. Annals of Applied Biology 39, 257–265. https://doi.org/10.1111/j.1744-7348.1952.tb00904.x.
Hoebeke, L., Bruffaerts, N., Verstraeten, C., Delcloo, A., Desmedt, T., et al., 2018. Thirty-four years of pollen monitoring: an evaluation of the temporal variation of pollen seasons in Belgium. Aerobiologia 34, 139. https://doi.org/10.1007/s10453-017-9503-5.
Khwarahma, N.R., Dash, J., Skjøth, C.A., Newnham, R.M., Adams-Groom, B., Heade, K., Caulton, E., Atkinson, P.M., 2017. Mapping the birch and grass pollen seasons in the UK using satellite sensor time-series. Sci. Total Environ. 578, 586–600.
KMI,https://www.meteo.be/nl/klimaat/klimaatverandering-in-belgie/klimaattrends-in-ukkel/luchttemperatuur/gemiddelde/lente (accessed on 9 March 2021).
Kouznetsov, R., Sofiev, M., 2012. A methodology for evaluation of vertical dispersion and dry deposition of atmospheric aerosols. J. Geophys. Res. 117 https://doi.org/10.1029/2011JD016366.
Landrigan, P.J. et al., 2017. The Lancet Commission on pollution and health. Published online October 19, 2017 10.1016/S0140-6736(17)32345-0.
Latvala, J., von Hertzen, L., Lindholm, H., Haahtela, T., 2005. Trends in prevalence of asthma and allergy in Finnish young men: nationwide study, 1966-2003. BMJ. https://doi.org/10.1136/bmj.38448.603924.AE.
Linkosalo, T., Ranta, H., Oksanen, A., Siljamo, P., Luomajoki, A., Kukkonen, J., et al., (2010). A double-threshold temperature sum model for predicting the flowering duration and relative intensity of Betula pendula and B. pubescens. Agricultural and Forest Meteorology, 150, 6–11. https://doi.org/10.1016/j.agrformet.2010.08.007.
Liu, C., Chen, R., Sera, F., et al., 2019. Ambient particulate air pollution and daily mortality in 652 cities. N. Engl J. Med. 381, 705–715. https://doi.org/10.1056/NEJMoa1817364.
Makra, L., Matyasovszky, I., Deak, A.J., 2011. Trends in the characteristics of allergenic pollen circulation in central Europe based on the example of Szeged, Hungary. Atmos. Environ. 45, 6010–6018.
Maya-Manzano, J.M., Smith, M., Markey, E., Hourihane, J., Clanct, O., Sodeau, J., OConnor, D.J., 2020. Recent developments in monitoring and modelling airborne pollen, a review. Grana. https://doi.org/10.1080/00173134.2020.1769176, 2020.
Maya-Manzano, J.M., Skjøth, C.A., Smith, M., Dowding, P., Sarda-Estève, R., Baisnée, D., McGillicuddy, E., Sewell, G., O'Connor, D.J., 2021. Spatial and temporal variations in the distribution of birch trees and airborne Betula pollen in Ireland. Agricul. Forest Meteorol. 298–299, 108298 https://doi.org/10.1016/j.agrformet.2020.108298.
Neumann, J.E., et al., 2019. Estimates of present and future asthma emergency department visits associated with exposure to oak, birch, and grass pollen in the United States. GeoHealth 3, 11–27.
Oteros, J., Buters, J., Laven, G., et al., 2017. Errors in determining the flow rate of Hirst-type pollen traps. Aerobiologia 33, 201–210. https://doi.org/10.1007/s10453-016-9467-x.
Pinzon, J.E., Tucker, C.J., 2014. A non-stationary 1981–2012 AVHRR NDVI3g time series. Remote Sens 6, 6929–6960.
Prank, M., Chapman, D.S., Bullock, J.M., Belmonte, J. et al., 2013. An operational model for forecasting ragweed pollen release and dispersion in Europe. Agricultural and Forest Meteorology, 182-183, 43–53, 10.1016/j.agrformet.2013.08.003.
Reitsma, S., Subramaniam, S., Fokkens, W.W., Wang, D.Y., 2018. Recent developments and highlights in rhinitis and allergen immunotherapy. Allergy 73, 2306–2313.
Ritenberga, O., Sofiev, M., Kirillova, V., Kalnina, L., Genikhovich, E., 2016. Statistical modelling of non-stationary processes of atmospheric pollution from natural sources: example of birch pollen. Agricul. Forest Meteorol., 226–227, 96–107, 10.1016/j.agrformet.2016.05.016.
Ritenberga, O., Sofiev, M., Siljamo, P., Saarto, A., Dahl, A., Ekebome, A., Sauliene, E., Shalaboda, V., Severova, E., Hoebeke, L., Ramfjord, H., 2018. A statistical model for predicting the inter-annual variability of birch pollen abundance in Northern and North-Eastern Europe. Sci. Total Environ. 615, 228–239.
Rojo, J., Oteros, J., Pérez-Badia, R., et al., 2019. Near-ground effect of height on pollen exposure. Environ. Res. 174, 160–169. https://doi.org/10.1016/j.envres.2019.04.027, 2019.
Savitzky, A., Golay, M.J.E., 1964. Smoothing and differentiation of data by simplified least squares procedures. Anal. Chem. 36 (8), 1627–1639.
Schmidt, C.W., 2016. Pollen overload: seasonal allergies in a changing climate. Environ. Health Perspect. 124, A71–A75.
Sen, P.K., 1968. Estimates of the regression coefficient based on Kendall's tau. J. Am. Stat. Assoc. 63 (324), 1379–1389. https://doi.org/10.2307/2285891.
Siljamo, P., Sofiev, M., Filatova, E., et al., 2013. A numerical model of birch pollen emission and dispersion in the atmosphere. Model evaluation and sensitivity analysis. Int. J. Biometeorol. 57, 125–136. https://doi.org/10.1007/s00484-012-0539-5.
Sofiev, M., Siljamo, P., Ranta, H., Rantio-Lehtimäki, A., 2006. Towards numerical forecasting of long-range air transport of birch pollen: theoretical considerations and a feasibility study. Int J. Biometeorology 50, 392–402. https://doi.org/10.1007/s00484-006-0027-x.
Sofiev, M., Siljamo, P., Ranta, H., Linkosalo, T., Jaeger, S., Rasmussen, A., Rantio-Lehtimaki, A., Severova, E., Kukkonen, J., 2013. A numerical model of birch pollen emission and dispersion in the atmosphere. Description of the emission module. Int. J. Biometeorol. 57, 45–58. https://doi.org/10.1007/s00484-012-0532-z.
Sofiev, M., Berger, U., Prank, M., Vira, J., Arteta, J., Belmonte, J., et al., 2015. MACC regional multi-model ensemble simulations of birch pollen dispersion in Europe. Atmos. Chem. Phys. 15, 8115–8130, 2015.
Stas, M., Aerts, R., Hendrickx, M., et al., 2021a. Exposure to green space and pollen allergy symptom severity: A case-crossover study in Belgium. Sci. Total Environ. 781 https://doi.org/10.1016/j.scitotenv.2021.146682.
Stas, M., Aerts, R., Hendrickx, M. et al., 2021b, Association between local airborne tree pollen composition and surrounding land cover across different spatial scales in Northern Belgium, Urban Forest. Urban Greening, 61, https://doi.org/10.1016/j.ufug.2021.127082.
Steckling-Muschack, N., Mertes, H., Mittermeier, I., et al., 2021. A systematic review of threshold values of pollen concentrations for symptoms of allergy. Aerobiologia. https://doi.org/10.1007/s10453-021-09709-4, 2021.
Tanentzap, A.J., Monks, A., 2018. Making the mast of a rainy day: environmental constraints can synchronize mass seeding across populations. New Phytologist 219, 6–8. https://doi.org/10.1111/nph.15219.
Taylor, K.E., 2001. Summarizing multiple aspects of model performance in a single diagram. J. Geophys. Res. 106, 7183–7192. https://doi.org/10.1029/2000JD900719.
Theil, H., 1950. A rank-invariant method of linear and polynomial regression analysis. I, II, III. Nederl. Akad. Wetensch., Proc. 53, 386–392, 521–525, 1397–1412.

Tucker, C.J., 1979. Red and photographic infrared linear combinations for monitoring vegetation. Remote Sens. Environ. 8, 127–150.
Verstraeten, W.W., Veroustraete, F., Feyen, J., 2006. On temperature and water limitation of net ecosystem productivity: Implementation in the C-Fix model. Ecolog. Mod. 199 (1), 4–22.
Verstraeten, W.W., Boersma, K.F., Douros, J., Williams, J.E., Eskes, H., Liu, F., Beirle, S., Delcloo, A., 2018. Top-down NOX emissions of European cities based on the downwind plume of modelled and space-borne tropospheric NO2 columns. Sensors 18, 2893. https://doi.org/10.3390/s18092893.
Verstraeten, W.W., Dujardin, S., Hoebeke, L., Bruffaerts, N., Kouznetsov, R., Dendoncker, N., Hamdi, R., Linard, C., Hendrickx, M., Sofiev, M., Delcloo, A.W., 2019. Spatio-temporal monitoring and modelling of birch pollen levels in Belgium. Aerobiologia 35 (4), 703–717. https://doi.org/10.1007/s10453-019-09607-w.
Verstraeten, W.W., Kouznetsov, R., Hoebeke, L., Bruffaerts, N., Sofiev, M., Delcloo, A.W., 2021. Modelling grass pollen levels in Belgium. Sci. Total Environ. 753, 141903 https://doi.org/10.1016/j.scitotenv.2020.141903.
WHO, 2003. Phenology and Human Health: Allergic Disorders.
Ziello, C., Sparks, T.H., Estrella, N., Belmonte, J., Bergmann, K.C., et al., 2012. Changes to airborne pollen counts across Europe. PLoS ONE 7 (4), e34076.
Ziska, L.H., Makra, L., Harry, S.K. et al., 2019. Temperature-related changes in airborne allergenic pollen abundance and seasonality across the northern hemisphere: a retrospective data analysis. The Lancet, 3 March 2019.